Quantum diffusion of light interstitials: One-phonon contribution to the impurity-lattice scattering

Philip D. Reilly,* Robert A. Harris, and K. Birgitta Whaley
Department of Chemistry, University of California at Berkeley, Berkeley, California 94720
(Received 29 May 1992; revised manuscript received 8 October 1992)

The dynamics of an impurity described by a single-band small-polaron model are investigated. In previous studies it was concluded that the lowest-order processes that can contribute to impurity-lattice scattering are two-phonon processes. We show that, for weak coupling, there is a one-phonon contribution to the scattering. The temperature of the site-to-site hopping rate is determined. We find that this one-phonon contribution gives a linear temperature dependence that can completely suppress the T^7 dependence predicted by the standard, two-phonon, analysis. Possible experimental manifestations of the one-phonon contribution are discussed.

I. INTRODUCTION

There are many physical systems whose low-temperature transport properties can be interpreted in terms of the quantum-mechanical tunneling of an impurity between interstitial sites of a host lattice. Some examples of such systems are μ^+ in metals,[1–7] muonium in NaCl and KCl,[8,9] hydrogen and deuterium in metals,[10–13] ortho-H_2 and HD in solid para-H_2,[14,15] ^{3}He in ^{4}He,[16–18] and hydrogen and its isotopes adsorbed on metal surfaces.[19–25] In these systems the mass transport of the impurities is thought to proceed *via* quantum-mechanical tunneling of the impurity from site to site, limited by scattering from the lattice, by scattering from other impurities, or by scattering from conduction electrons.

For the systems described above it is assumed that the amplitude of tunneling from site to site is small compared to other energies in the system, e.g., the Debye frequency of the host lattice, and the vibrational frequency of an impurity on one site. If the tunneling between sites is treated as a perturbation, the model is called a small polaron model for the narrow band transport. This model was originally proposed in order to explain electron conduction in narrow band materials.[26] It has also been applied to the theory of the quantum diffusion of light interstitials in solids,[27–30] the quantum diffusion of light adsorbates on surfaces,[31–34] and to the transport properties of excitons.[35–38]

The low-temperature transport properties of the experimental systems listed above all show a temperature dependence that is indicative of weak coupling between the impurity and the lattice (or the conduction electrons). For weak coupling of the impurity to the host lattice, the standard analysis of the small-polaron model predicts that the lowest-order processes that can contribute to impurity-lattice scattering are two-phonon processes.[26,27] These processes are strongly temperature dependent, with a site-to-site hopping rate predicted to go as T^7 at low temperatures for tunneling in a three-dimensional (3D) system. However, such strong power-law dependence is not seen experimentally.[39]

In this paper we show that there are one-phonon processes that contribute to the impurity-lattice scattering when the impurity is tunneling between identical, degenerate sites, i.e., the situation described by the standard small-polaron model. This is the main result of this paper. In previous work the site-localized impurity states were treated as stationary states of the thermally averaged Hamiltonian, and the hopping rate between these states was calculated using perturbation theory.[26–28] However, the thermally averaged Hamiltonian includes site-to-site tunneling operators which mix the site-localized states, and therefore these states cannot be treated as stationary states. When this nonstationarity of the localized states is included in the calculation of the rates, we find that it is possible to get a one-phonon contribution to the impurity-lattice scattering.

At low temperatures the one-phonon contribution to the scattering has a profound effect on both the magnitude and the temperature dependence of the impurity, site-to-site, hopping rate. The one-phonon contribution shows a linear temperature dependence which can completely suppress the T^7 temperature dependence predicted by the standard two-phonon scattering. Indeed, we will show that the standard T^7 result can only be seen for systems in which the impurity bands are extremely narrow, in which case the one-phonon contribution becomes negligible. Exactly what we mean by "extremely narrow" will be made quantitative in the body of the paper.

The lack of experimental observation of the strong two-phonon temperature dependence may be due to the fact that for such extremely narrow bands, either (i) the tunneling rates, and hence any transport properties, become immeasurably small, or, (ii) that the imperfections of any real lattice are enough to cause site-energy asymmetries greater than the impurity bandwidth. In the latter case an alternative one-phonon mechanism, which we will discuss in Sec. IV, will operate and this also gives rise to a linear temperature dependence.[40]

In Sec. II, we present the small-polaron model and analyze the dynamics of the impurity using the equations of motion of the reduced density matrix. The temperature dependence of the impurity site-to-site hopping rate is reported in Sec. III. We compare our results to the standard two-phonon results and show under what conditions

the standard analysis is applicable. In Sec. IV, we compare the one-phonon contribution that arises out of our analysis with the results for other possible one-phonon mechanisms. We also speculate on possible experimental manifestations of this new one-phonon contribution to the scattering. In Sec. V, we briefly summarize the main results of this paper.

II. HAMILTONIAN AND EQUATION OF MOTION OF REDUCED DENSITY MATRIX

The single-band Hamiltonian for noninteracting interstitial impurities moving in a periodic lattice and coupled linearly to the lattice displacements is

$$H=-t_0\sum_{\mathbf{s},\mathbf{n}}a_{\mathbf{s}}^{\dagger}a_{\mathbf{s}+\mathbf{n}}+\sum_{\mathbf{q}}\omega_{\mathbf{q}}b_{\mathbf{q}}^{\dagger}b_{\mathbf{q}} +\sum_{\mathbf{s}}n_{\mathbf{s}}\sum_{\mathbf{q}}(\gamma_{\mathbf{s},\mathbf{q}}b_{\mathbf{q}}+\gamma_{\mathbf{s},\mathbf{q}}^{*}b_{\mathbf{q}}^{\dagger}) . \tag{2.1}$$

Here $\mathbf{s}$ labels the sites in the lattice, $\mathbf{n}$ the nearest-neighbor sites, and $\mathbf{q}$ the phonon modes. $a_{\mathbf{s}}^{\dagger}$ ($a_{\mathbf{s}}$) creates (destroys) an impurity at site $\mathbf{s}$, $n_{\mathbf{s}}$ ($=a_{\mathbf{s}}^{\dagger}a_{\mathbf{s}}$) is the number operator for this state and $b_{\mathbf{q}}^{\dagger}$ ($b_{\mathbf{q}}$) creates (destroys) a phonon in normal mode $\mathbf{q}$ with frequency $\omega_{\mathbf{q}}$ ($\mathbf{q}$ labels both wave vector and polarization branch). t_0 is the bare tunneling amplitude. This Hamiltonian is derived assuming that the lattice can only connect impurity states on the same site. Therefore, the impurity-lattice coupling is through the impurity density only, with strength $\gamma_{\mathbf{s},\mathbf{q}}$. There is also the implicit assumption that the tunneling amplitude between nearest-neighbor sites, t_0, is much greater in magnitude than any difference in site energies. In the Hamiltonian, Eq. (2.1) all site energies are taken to be equal and are set to zero. For any real system this last assumption will become more questionable as the mass of the tunneling impurity increases. Eventually any site-energy asymmetry, due to lattice imperfections or interaction with other interstitials, will be enough to cause the zero-order impurity eigenstates to become localized. We assume that the tunneling amplitude, t_0, is large enough that the site-energy differences can be ignored but that it is still small compared with the maximum lattice frequency, $\omega_{\max}$.

The standard polaron transformation[41]

$$U=\exp\left[-\sum_{\mathbf{s}}n_{\mathbf{s}}\sum_{\mathbf{q}}\left[\frac{\gamma_{\mathbf{s},\mathbf{q}}}{\omega_{\mathbf{q}}}b_{\mathbf{q}}-\frac{\gamma_{\mathbf{s},\mathbf{q}}^{*}}{\omega_{\mathbf{q}}}b_{\mathbf{q}}^{\dagger}\right]\right] , \tag{2.2}$$

of the Hamiltonian, Eq. (2.1), gives

$$UHU^{\dagger}=-t_0\sum_{\mathbf{s},\mathbf{n}}B_{\mathbf{s},\mathbf{s}+\mathbf{n}}a_{\mathbf{s}}^{\dagger}a_{\mathbf{s}+\mathbf{n}}+\sum_{\mathbf{q}}\omega_{\mathbf{q}}b_{\mathbf{q}}^{\dagger}b_{\mathbf{q}}-\sum_{\mathbf{s},\mathbf{s}'}V_{\mathbf{s},\mathbf{s}'}n_{\mathbf{s}}n_{\mathbf{s}'} \tag{2.3}$$

with

$$B_{\mathbf{s},\mathbf{s}+\mathbf{n}}=\exp\left[-\sum_{\mathbf{q}}(\Delta_{\mathbf{q}}^{\mathbf{s},\mathbf{s}+\mathbf{n}}b_{\mathbf{q}}-\Delta_{\mathbf{q}}^{\mathbf{s},\mathbf{s}+\mathbf{n}*}b_{\mathbf{q}}^{\dagger})\right] \tag{2.3a}$$

and

$$\Delta_{\mathbf{q}}^{\mathbf{s},\mathbf{s}+\mathbf{n}}=\frac{\gamma_{\mathbf{s},\mathbf{q}}-\gamma_{\mathbf{s}+\mathbf{n},\mathbf{q}}}{\omega_{\mathbf{q}}}=\frac{\gamma_{\mathbf{q}}}{\omega_{\mathbf{q}}}e^{i\mathbf{q}\cdot\mathbf{s}}(1-e^{i\mathbf{q}\cdot\mathbf{n}}) . \tag{2.3b}$$

The last term in Eq. (2.3) is a lattice-induced impurity-impurity interaction with strength $V_{\mathbf{s},\mathbf{s}'}$ given by

$$V_{\mathbf{s},\mathbf{s}'}=\sum_{\mathbf{q}}\frac{\mathrm{Re}[\gamma_{\mathbf{s}\mathbf{q}}\gamma_{\mathbf{s}'\mathbf{q}}^{*}]}{\omega_{\mathbf{q}}} . \tag{2.3c}$$

In the limit of dilute impurities we can ignore these lattice-induced interactions between the impurities. We therefore retain only the diagonal elements of $V_{\mathbf{s},\mathbf{s}'}$, which add a site-independent, lattice-induced stabilization. In this limit the transformed Hamiltonian becomes

$$UHU^{\dagger}=-t_0\sum_{\mathbf{s},\mathbf{n}}B_{\mathbf{s},\mathbf{s}+\mathbf{n}}a_{\mathbf{s}}^{\dagger}a_{\mathbf{s}+\mathbf{n}}+\sum_{\mathbf{q}}\omega_{\mathbf{q}}b_{\mathbf{q}}^{\dagger}b_{\mathbf{q}}-E_{\mathrm{stab}}\sum_{\mathbf{s}}n_{\mathbf{s}} , \tag{2.4}$$

where

$$E_{\mathrm{stab}}=V_{\mathbf{s},\mathbf{s}}=\sum_{\mathbf{q}}\frac{|\gamma_{\mathbf{q}}|^2}{\omega_{\mathbf{q}}} . \tag{2.4a}$$

In deriving these results we have used the periodicity of the lattice in order to write the coupling strength $\gamma_{\mathbf{s},\mathbf{q}}$ in the form

$$\gamma_{\mathbf{s},\mathbf{q}}=\gamma_{\mathbf{q}}e^{i\mathbf{q}\cdot\mathbf{s}} . \tag{2.5}$$

The $\mathbf{q}$ dependence of $\gamma_{\mathbf{q}}$ will depend on the dimensionality of the phonon system and on the details of the impurity-lattice coupling.

The dynamics generated by the Hamiltonian in Eq. (2.4) will be analyzed using perturbation theory, treating the tunneling as the perturbation. We therefore take the last two terms of Eq. (2.4) as our zero-order Hamiltonian, H_0. The tunneling terms, which now include the lattice operators $B_{\mathbf{s},\mathbf{s}+\mathbf{n}}$, provide the perturbation V. That is

$$UHU^{\dagger}=H_0+V \tag{2.6}$$

with

$$H_0=-E_{\mathrm{stab}}\sum_{\mathbf{s}}n_{\mathbf{s}}+\sum_{\mathbf{q}}\omega_{\mathbf{q}}b_{\mathbf{q}}^{\dagger}b_{\mathbf{q}} \tag{2.6a}$$

and

$$V=-t_0\sum_{\mathbf{s},\mathbf{n}}B_{\mathbf{s},\mathbf{s}+\mathbf{n}}a_{\mathbf{s}}^{\dagger}a_{\mathbf{s}+\mathbf{n}} . \tag{2.6b}$$

The Hamiltonian given in Eq. (2.6) describes a small-polaron model for interstitial motion in the limit of dilute interstitials. This Hamiltonian has been extensively studied in a variety of contexts, some of which have been discussed in the Introduction.

The dynamics of this coupled many-body quantum systems are, for our purposes, best analyzed by looking at the equations of motion of the reduced density matrix in the site basis. For an impurity whose motion is described by the Hamiltonian given in Eq. (2.6), the equations of motion, in the Markovian approximation, are given by[42,43]

$$\dot{\bar{\rho}}_{s,s'}(t)=i\tilde{t}_0\sum_n[\bar{\rho}_{s+n,s'}(t)-\bar{\rho}_{s,s'+n}(t)] -z\gamma^-\bar{\rho}_{s,s'}(t)+\delta_{s',s}\sum_n\gamma^-\bar{\rho}_{s+n,s+n}(t) +\sum_n\delta_{s',s+n}\gamma^+\bar{\rho}_{s',s}(t)\ , \tag{2.7}$$

where z is the number of nearest-neighbor sites. $\tilde{t}_0$ is the renormalized tunneling amplitude and can be written as

$$\tilde{t}_0=\theta t_0 \tag{2.8}$$

with the renormalizing factor θ given by

$$\theta=\exp\left[-\frac{1}{2}\int_0^1 d\omega\frac{J(\omega)}{\omega^2}\coth\left[\frac{\omega}{2kT/\omega_{\max}}\right]\right]\ . \tag{2.8a}$$

$J(\omega)$ appearing in Eq. (2.8a) is a dimensionless spectral weight function defined by

$$J(\omega)\equiv 4\sum_{\mathbf{q}}\frac{|\gamma_{\mathbf{q}}|^2}{\omega_{\max}^2}\sin^2(\mathbf{q}\cdot\mathbf{n}/2)\delta(\omega-\omega_{\mathbf{q}}/\omega_{\max})\ . \tag{2.9}$$

γ^- appearing in Eq. (2.7) is the "Golden Rule" rate of impurity transfer from one site to a neighboring site, i.e., the impurity site to site hopping rate. γ^- and γ^+ can be written as[43]

$$\gamma^{\pm}=\omega_{\max}t_0^2\tilde{\gamma}^{\pm} \tag{2.10}$$

with dimensionless rates $\tilde{\gamma}^{\pm}$ given by

$$\tilde{\gamma}^{\pm}=e^{-\phi(0)}\int_{-\infty}^{\infty}d\tau J_0^{2d}(2\tilde{t}_0\tau)[e^{\mp\phi(\tau)}-1] \tag{2.11}$$

and

$$\phi(\tau)=\int_0^1 d\omega\frac{J(\omega)}{\omega^2}[\coth(\omega/2kT)\cos(\omega\tau)-i\sin(\omega\tau)]\ . \tag{2.12}$$

The tunneling amplitude, t_0, and temperature kT, appearing in Eqs. (2.10)–(2.12) are now dimensionless and are in units of the maximum lattice frequency, $\omega_{\max}$. d appearing in Eq. (2.11) is the dimensionality of the tunneling system and J_0 is the zero-order Bessel function. The standard small-polaron expression for γ^- is the same as given in Eqs. (2.10)–(2.12) except that it does not contain the $J_0^{2d}(2\tilde{t}_0\tau)$ factor.[27] The appearance of this extra factor is a consequence of the correct inclusion of the nonstationarity of the site-localized states in the calculation of the site-to-site hopping rates.[43] If γ^- and γ^+ are calculated using the standard small-polaron expression, i.e., setting $J_0^{2d}(2\tilde{t}_0\tau)=1$, the equation of motion given in Eq. (2.7) reduces to the result previously obtained by Kitahara *et al.*[31]

III. TEMPERATURE DEPENDENCE OF THE HOPPING RATES

We now investigate the temperature dependence of the dimensionless rates given in Eq. (2.11). For weak impurity-lattice coupling the contribution of many-phonon processes to these rates is unimportant, and we may expand the integrand to obtain a series of terms corresponding to one-phonon processes, two-phonon processes, etc.,

$$\tilde{\gamma}^{\pm}=e^{-\phi(0)}\int_{-\infty}^{\infty}d\tau J_0^{2d}(2\tilde{t}_0\tau) \times\{\mp\phi(\tau)+\tfrac{1}{2}[\phi(\tau)]^2\mp\cdots\}\ . \tag{3.1}$$

Interchanging the order of the time and frequency integration in Eq. (3.1) we obtain

$$\tilde{\gamma}^{\pm}=e^{-\phi(t)}(\mp\gamma^{(1)}+\gamma^{(2)}\mp\cdots)\ , \tag{3.2}$$

where $\gamma^{(n)}$ represents the n-phonon contribution to the rate. The one- and two-phonon terms are given by

$$\gamma^{(1)}=\int_0^1 d\omega\frac{J(\omega)}{\omega^2}\coth(\omega/2kT)F(\omega) \tag{3.3}$$

and

$$\gamma^{(2)}=\frac{1}{4}\int_0^1 d\omega_1\int_0^1 d\omega_2\frac{J(\omega_1)}{\omega_1^2}\frac{J(\omega_1)}{\omega_2^2}\{[\coth(\omega_1/2kT)\coth(\omega_2/2kT)-1]F(\omega_1-\omega_2) +[\coth(\omega_1/2kT)\coth(\omega_2/2kT)+1]F(\omega_1+\omega_2)\} \tag{3.4}$$

with

$$F(\omega)=\int_{-\infty}^{\infty}d\tau J_0^{2d}(2\tilde{t}_0\tau)\cos(\omega\tau)\ . \tag{3.5}$$

Before investigating the effects of the nonstationarity of the site-localized states on these rates we will review the standard results[26–28] obtained by setting the Bessel functions in Eq. (3.5) equal to unity. $F(\omega)$ then becomes proportional to a δ function at zero frequency. In analyzing these terms we will restrict ourselves to spectral weight functions with the model form

$$J(\omega)=\begin{cases}\eta\omega^n, & \omega\le 1\ ,\\ 0, & \omega>1\ .\end{cases} \tag{3.6}$$

The value of η, which we will call the coupling strength, will depend on the strength of the impurity-lattice interaction. The frequency exponent, n, will depend on the dimensionality of the lattice and on the details of the local impurity-lattice interactions. For an interstitial tunneling between identical sites in a three-dimensional solid $J(\omega)\sim\omega^5$.[34,43,44]

Using the spectral weight function given in Eq. (3.6), with $n=5$, the standard one- and two-phonon contributions to the rate become

$$\gamma^{(1)}=0 \tag{3.7}$$

and

$$\gamma^{(2)}=\eta^2\frac{\pi}{2}(2kT)^7\int_0^{1/(2kT)}d\omega\frac{\omega^6}{\sinh^2(\omega)} \ . \tag{3.8}$$

Equation (3.7) states that, in the standard picture, conservation of energy requires that there are no one-phonon processes that contribute to the site-to-site hopping rate.[26,27] For low enough temperatures the upper limit of the integration in Eq. (3.8) can be taken to infinity, yielding standard integrals.[45] In this limit the two-phonon contribution becomes

$$\gamma^{(2)}=\eta^2\frac{(2\pi)^7}{84}(kT)^7 \quad (2kT\ll 1) \ . \tag{3.9}$$

As long as the temperature dependence of the renormalizing factor $e^{-\phi(0)}$ is not too strong, the overall temperature dependence of the rate, at low temperatures, goes as T^7. For higher temperature we can approximate the integrand in Eq. (3.8) by its leading-order term. This then yields a T^2 temperature dependence for the two-phonon contribution

$$\gamma^{(2)}=\eta^2\frac{2\pi}{5}(kT)^2 \quad (2kT\geq 1) \ . \tag{3.10}$$

When the time dependence of $J_0^{2d}(2\tilde{t}_0\tau)$ is included in the calculation of the rates, $F(\omega)$ is no longer proportional to a δ function. $F(\omega)$ can be calculated analytically for 1D,[46] and for 2D and 3D it was integrated numerically. In Fig. 1, we show plots of the function $F(\omega)$ for one-, two-, and three-dimensional tunneling systems. The effect of including the $J_0^{2d}(2\tilde{t}_0\tau)$ factor is to smear out the zero-frequency δ function, giving it a width equal to twice the renormalized bandwidth. For 2D and 3D systems $F(\omega)$ is identically equal to zero for $\omega>8\tilde{t}_0$ and $\omega>12\tilde{t}_0$, respectively.

In the Appendix we calculate the one-phonon and two-phonon contributions to the rate for a 3D tunneling system coupled to a 3D lattice, i.e., $J(\omega)=\eta\omega^5$ and $F(\omega)$ given in Fig. 1(c). The results are

$$\gamma^{(1)}\approx\begin{cases}\eta^2\left[\dfrac{\tilde{t}_0^2}{\eta}\right]\tilde{t}_0\dfrac{\xi 12^4}{\sqrt{2}}, & kT\ll 6\tilde{t}_0 \ , \\ \eta^2\left[\dfrac{\tilde{t}_0^2}{\eta}\right]\dfrac{125\sqrt{2\pi}}{4}kT, & kT\gg 6\tilde{t}_0 \ ,\end{cases} \tag{3.11}$$

and

$$\gamma^{(2)}\approx\begin{cases}\eta^2\dfrac{(2\pi)^7}{84}(kT)^7, & 2kT\ll 1 \ , \\ \eta^2\dfrac{2\pi}{5}(kT)^2, & 2kT\geq 1 \ .\end{cases} \tag{3.12}$$

The utility of writing the one-phonon contribution in terms of the ratio $\tilde{t}_0^2/\eta$ will be made clear shortly. ξ appearing in the low-temperature limit of Eq. (3.11) is defined by

$$\xi\equiv\sum_{n=0}^{\infty}\frac{(-1)^n}{n!}\frac{(2.4)^{2n}}{(4+2n)}\sim 1.4749\times 10^{-2} \ . \tag{3.13}$$

From Eq. (3.11) we see that when the nonstationarity of the site-localized states is included in the calculation of the rates we now get a one-phonon contribution. The nonstationarity of the localized states leads to an uncertainty in their energy (of the order of the renormalized bandwidth). It is therefore possible to get a one-phonon contribution to the rate without violating conservation of energy.

At low temperatures the one-phonon contribution will

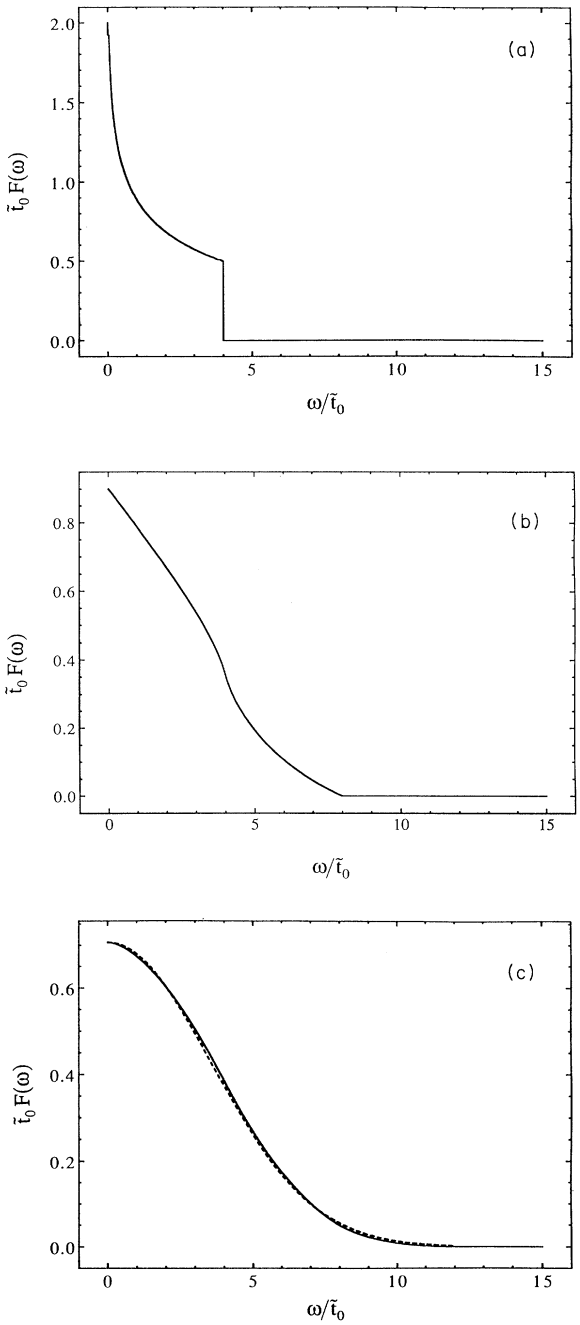

FIG. 1. Function $F(\omega)$ [Eq. (3.5)] (multiplied by renormalized tunneling amplitude $\tilde{t}_0$) as function of frequency (in units of $\tilde{t}_0$). (a) 1D tunneling system, (b) 2D tunneling system, (c) 3D tunneling system. The dashed curve is the approximation given in Eq. (A1).

dominate and will give rise to nonstandard temperature and isotope dependence for the rate. Both $\gamma^{(1)}$ and $\gamma^{(2)}$ are monotonic increasing functions of temperature, and the temperature exponent of $\gamma^{(1)}$ is always less than that of $\gamma^{(2)}$. We can therefore find a unique temperature, denoted kT^*, below which the one-phonon rate exceeds the two-phonon rate. This transition temperature is given by

$$kT^* \approx \begin{cases} \left[\dfrac{\tilde{t}_0^2}{\eta}\right]^{1/6} 0.507\,18, & 2kT^* \ll 1 , \\ \dfrac{\tilde{t}_0^2}{\eta} 62.3346, & 2kT^* \geq 1 . \end{cases} \tag{3.14}$$

In Fig. 2 we show a representative plot of the temperature dependence of the full rate, calculated by numerical integration of Eq. (2.11). For temperatures below kT^* the full rate is very different from the standard T^7 rate. The temperature dependence now shows four distinct temperature regimes.

(i) At the lowest temperatures, $kT \leq t_0$, the rate is temperature independent, and is given by the low temperature limit of Eq. (3.11).

(ii) For $6t_0 \leq kT \leq kT^*$ we see a linear temperature dependence, due to the high-temperature limit of the one-phonon contribution, Eq. (3.11).

(iii) For temperatures above kT^*, the two-phonon contribution dominates. In the regime $kT^* \leq kT \leq \frac{1}{4}$ the temperature exponent is somewhat less than the T^7 predicted by the standard treatment.

(iv) Finally, at the highest temperatures, $\frac{1}{2} \leq kT$, we go over to the T^2 high-temperature limit of the two-phonon rate.

Inclusion of the one-phonon contribution has a profound effect on the low-temperature behavior of the rate. For the lowest temperatures shown in Fig. 2 the full rate is 13 orders of magnitude greater than that predicted by the standard T^7 result.

In Fig. 3 we show how the ratio t_0^2/η affects the temperature dependence of the rate, $\tilde{\gamma}^-$, for two different values of the coupling strength, η. The temperature dependence of the scaled rate depends on the ratio t_0^2/η in three ways: (i) the low-temperature value scales as t_0^2/η, Eq. (3.11); (ii) the transition temperature, kT^*, is determined by t_0^2/η through Eq. (3.14); and (iii) the temperature exponent in the intermediate-temperature regime $kT^* \leq kT \leq \frac{1}{4}$ depends on t_0^2/η. Writing the temperature dependence of the rate in the intermediate regime as $\tilde{\gamma}^- \sim T^\kappa$, Fig. 4 and Table I show the dependence of the temperature exponent, κ, on the ratio t_0^2/η. In Fig. 4, we show the best fits for κ, for the parameters $t_0^2/\eta = 10^{-4}$ and 10^{-6}, and in Table I we summarize the dependence of κ on t_0^2/η. From Fig. 4 and Table I we see that the intermediate-temperature dependence is well described by $\tilde{\gamma}^- \sim T^\kappa$, with κ given approximately by

$$\kappa \approx \begin{cases} -\log_{10}(\tilde{t}_0^2/\eta), & \tilde{t}_0^2/\eta \geq 10^{-7} , \\ 7, & \tilde{t}_0^2/\eta < 10^{-7} . \end{cases} \tag{3.15}$$

We will therefore only see the standard T^7 temperature dependence if we are in a parameter regime for which $\tilde{t}_0^2/\eta < 10^{-7}$, i.e., very narrow bands.

In summary, for weak impurity-lattice coupling the main effect of including the nonstationarity of the site-localized states in the calculation of the site-to-site hopping rate, i.e., including the $J_0^{2d}(2\tilde{t}_0\tau)$ factor in Eq. (3.5), is to allow a contribution from one-phonon processes. These processes completely change the low-temperature behavior of the rate from that predicted by the standard, weak-coupling, two-phonon rate which goes as T^7 in 3D.

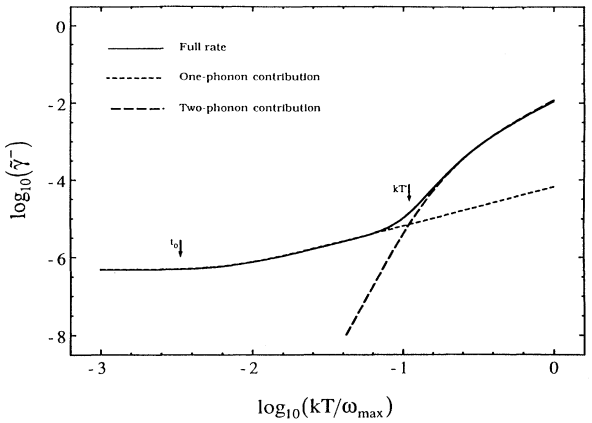

FIG. 2. Log-log plot of the dimensionless rate, $\tilde{\gamma}^-$ [Eq. (2.11)], as a function of temperature (in units of ω_{max}) (solid curve). Calculated for a 3D system, i.e., $J(\omega)=\eta\omega^5$ and $F(\omega)$ given in Fig. 1(c), with $\eta=10^{-1}$ and $t_0=10^{-2.5}$, i.e., $t_0^2/\eta=10^{-4}$. The transition temperature, kT^*, is defined in Eq. (3.14). Also plotted are the one-phonon (short-dashed curve) and two-phonon (long-dashed curve) contributions.

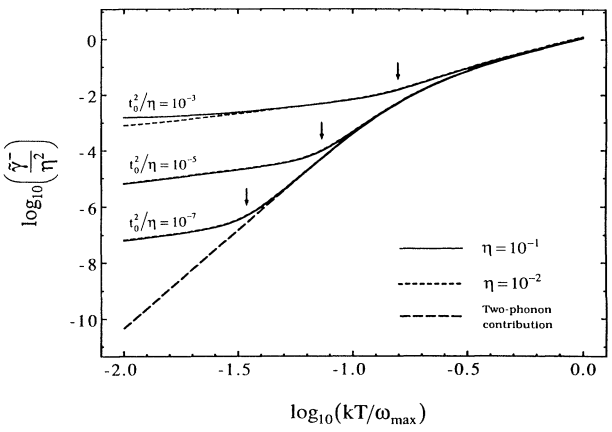

FIG. 3. Log-log plot of the dimensionless rate, $\tilde{\gamma}^-$ [Eq. (2.11)] (in units of η^2) as a function of temperature (in units of ω_{max}). Calculated for a 3D system, i.e., $J(\omega)=\eta\omega^5$ and $F(\omega)$ given in Fig. 1(c), with $\eta=10^{-1}$ and 10^{-2}, and $t_0^2/\eta=10^{-3}$, 10^{-5}, and 10^{-7}. Arrows indicate the transition temperature, kT^*, defined in Eq. (3.14). Also shown is the two-phonon contribution to the rate.

TABLE I. Dependence of the temperature exponent, κ, on the ratio t_0^2/η, for a 3D tunneling system coupled to a 3D lattice.

t_0^2/η	κ	Valid for $kT\sim$
10^{-3}	2.57	0.16–0.40
10^{-4}	4.00	0.11–0.25
10^{-5}	5.20	0.063–0.16
10^{-6}	6.06	0.056–0.14
10^{-7}	6.48	0.040–0.10
10^{-8}	6.79	0.032–0.10

At low temperatures the rate is dominated by the one-phonon contribution, and shows a linear dependence on temperature. The one-phonon contribution can also modify the T^7 temperature dependence, due to the two-phonon processes at higher temperatures. For intermediate temperatures, $kT^* \leq kT \leq 2.5kT^*$, the temperature dependence can range from T^7 to T^2. The exact power-law dependence is determined by the ratio t_0^2/η. The one- and two-phonon contributions to the rate $\gamma^{(1)}$ and $\gamma^{(2)}$ and the transition temperature kT^* for a 2D tunneling system coupled to a 2D lattice are given in the Appendix.

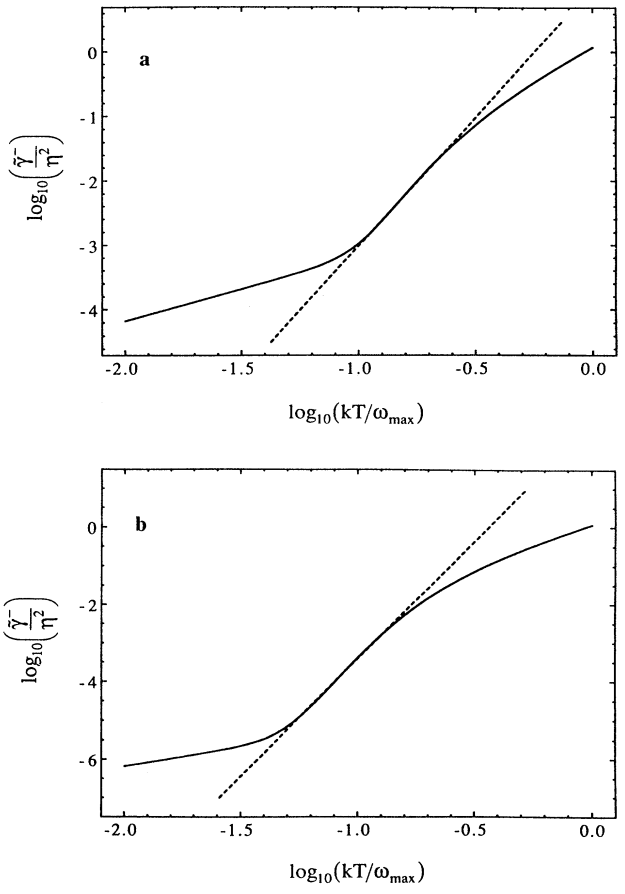

FIG. 4. Log-log plot of the dimensionless rate, $\tilde{\gamma}^-$ [Eq. (2.11)], (in units of η^2) as a function of temperature (in units of ω_{max}) (solid curve) and best linear fit to the log-log plot in the intermediate-temperature range (dashed curve). Calculated for a 3D system, i.e., $J(\omega)=\eta\omega^5$ and $F(\omega)$ given in Fig. 1(c), with (a) $t_0^2/\eta=10^{-4}$, (b) $t_0^2/\eta=10^{-6}$.

IV. COMPARISON TO OTHER ONE-PHONON MECHANISMS AND TO EXPERIMENT

A. Comparison to other one-phonon mechanisms

The one-phonon contribution to the site-to-site hopping rate derived in this paper is given by

$$\gamma^- = \omega_{max}\tilde{t}_0^2\gamma^{(1)} , \tag{4.1}$$

where $\gamma^{(1)}$ is defined in Eq. (3.3). For a 3D tunneling system the high- and low-temperature limits of $\gamma^{(1)}$ are given in Eq. (3.11) and these then give a one-phonon contribution to the rate of

$$\gamma^- \approx \begin{cases} \omega_{max}\eta\tilde{t}_0^5 216.26, & kT \leq \tilde{t}_0 , \\ \omega_{max}\eta\tilde{t}_0^4 78.33kT, & kT \geq 6\tilde{t}_0 . \end{cases} \tag{4.2}$$

There are two other slightly different physical situations which can given rise to one-phonon contributions to the site-to-site hopping rate. The first occurs if the interstitial sites are not degenerate and the site-energy differences between adjacent sites is much greater than the tunneling amplitude.[40] The Hamiltonian describing such a system is given by

$$H = \sum_s \varepsilon_s n_s - t_0 \sum_{s,n} a_s^\dagger a_{s+n} + \sum_q \omega_q b_q^\dagger b_q + \sum_s n_s \sum_n (\gamma_{s,q} b_q + \gamma_{s,q}^* b_q^\dagger) , \tag{4.3}$$

where ε_s is the impurity energy on site **s**, and $|\varepsilon_s - \varepsilon_{s'}| \gg t_0$ for all nearest-neighbor pairs of sites **s** and **s'**. This Hamiltonian is the same as the original Hamiltonian given in Eq. (2.1) except for the additional site energy term, $\sum_s \varepsilon_s n_s$. Since $|\varepsilon_s - \varepsilon_{s'}| \gg t_0$, the site-localized states are good zero-order eigenstates. Assuming that the spectral weight function is given by $J(\omega)=\eta\omega^5$, the Golden Rule rate of going from site **s** to site **s**+**n** is given by

$$\gamma_{s\to s+n}^- = 2\pi\omega_{max}\eta\tilde{t}_0^2\Delta\varepsilon^3 \begin{cases} \coth(\Delta\varepsilon/2kT)+1, & \varepsilon_s > \varepsilon_{s+n} , \\ \coth(\Delta\varepsilon/2kT)-1, & \varepsilon_s < \varepsilon_{s+n} , \end{cases} \tag{4.4}$$

with

$$\Delta\varepsilon = |\varepsilon_{s+n} - \varepsilon_s| . \tag{4.4a}$$

In Eq. (4.4), the site energies, tunneling amplitude, and temperature are all dimensionless and are given in units of the maximum lattice frequency, ω_{max}. For low temperatures, $kT \ll \Delta\varepsilon$, we can replace $\coth(\Delta\varepsilon/2kT)$ in Eq. (4.4) by unity, yielding

$$\gamma_{s\to s+n}^-(kT \ll \Delta\varepsilon) = \begin{cases} \omega_{max}\eta\tilde{t}_0^2\Delta\varepsilon^3 4\pi, & \varepsilon_s > \varepsilon_{s+n} , \\ 0, & \varepsilon_s < \varepsilon_{s+n} . \end{cases} \tag{4.5}$$

For temperatures greater than $\Delta\varepsilon$ the uphill ($\varepsilon_s < \varepsilon_{s+n}$) and downhill ($\varepsilon_s > \varepsilon_{s+n}$) rates become equal and are given

by

$$\gamma^{-}_{s\to s+n}(kT \gg \Delta\varepsilon)=\omega_{\max}\eta\tilde{t}_0^2\Delta\varepsilon^2 4\pi kT \ . \tag{4.6}$$

These one-phonon rates are similar to the rates given in Eq. (4.2) except that the form of the temperature dependence is now determined by the site-energy asymmetry, $\Delta\varepsilon$, and the magnitude of the rate depends on both $\Delta\varepsilon$ and $\tilde{t}_0$. The purity of the sample, the number of defects, and the concentration of the tunneling impurities can all affect the value of $\Delta\varepsilon$. We therefore expect that the observed transport properties will depend on all of these factors.

A second one-phonon contribution to the hopping rate is possible if the tunneling occurs between inequivalent sites within a unit cell.[40] In this case we will get a one-phonon contribution even when the inequivalent sites are degenerate. For a 3D system this intraunit-cell tunneling will be described by a spectral weight function that goes as ω^3 at low frequencies, i.e.,

$$J_{\text{intra}}(\omega)=\begin{cases}\tilde{\eta}\omega^3, & \omega<1 \ , \\ 0, & \omega>1 \ .\end{cases} \tag{4.7}$$

We have written the coupling strength in Eq. (4.7) as $\tilde{\eta}$ to emphasize the fact that the coupling to the lattice for these intraunit-cell processes is different than that which leads to the ω^5 spectral weight used in this paper. $\tilde{\eta}$ will only be nonzero if there is some change in the trace of the double force tensor in going from site to site within the unit cell.[2,40] With an ω^3 spectral weight function the standard analysis, i.e., taking $J_0^{2d}(2\tilde{t}_0\tau)=1$ in Eq. (3.5), yields a one-phonon contribution to the rate. In this case the one-phonon contribution is given by

$$\gamma^{-}_{\text{intra}}=\omega_{\max}\tilde{\eta}\tilde{t}_0^2\lim_{\omega\to 0}[2\pi\omega\coth(\omega/2kT)] \ , \tag{4.8}$$

which upon taking the zero-frequency limit gives

$$\gamma^{-}_{\text{intra}}=\omega_{\max}\tilde{\eta}\tilde{t}_0^2 4\pi kT \ . \tag{4.9}$$

The intraunit-cell mechanism gives rise to a one-phonon rate which is proportional to T for all temperatures. This is very different from the rate given in Eq. (4.2) which predicts a finite hopping rate at $T=0$. This difference should, in principle, make it possible to distinguish between these two one-phonon mechanisms. We now examine some experimental results on the transport properties of light interstitials in 3D which might be explained in terms of a one-phonon impurity-lattice scattering mechanism.

B. Comparison to experiment

1. *Diffusion of positive muons in aluminum*

A linear temperature dependence of the hopping rate has been observed in experiments on μ^+ diffusion in metals[1,2,4,6,7] and it has been speculated that this temperature dependence is due to one-phonon muon-lattice scattering.[1,2,4,6–8] In Fig. 5 we show the experimental data for μ^+ diffusion in aluminum[1,47] together with a representative fit of the data using our one- and two-phonon model. The experiments measure the rate of site-to-site μ^+ transfer, which is referred to as the hopping rate ν, and are fit using our calculated hopping rate γ^-, given in Eq. (2.10). Above about 4 K the experimentally observed hopping rate is an increasing function of temperature, with two distinct temperature regimes. At intermediate temperatures, between about 4 and 40 K, the rate is a nearly linear function of the temperature, while at higher temperatures there is a much stronger temperature dependence. For temperatures between about 40 and 100 K the hopping rate is well described by a power-law temperature dependence, $\nu\propto T^{\kappa}$, with $\kappa\approx 4.7$.

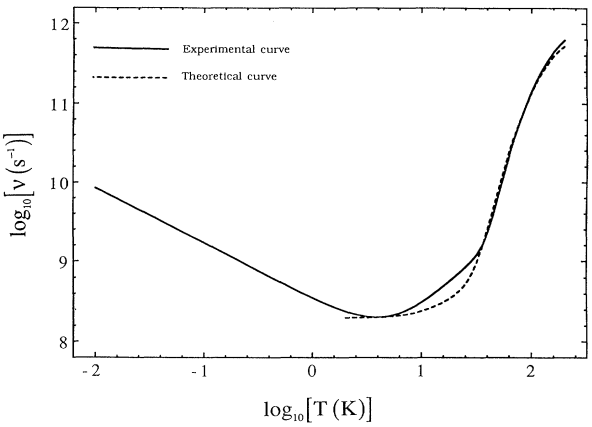

FIG. 5. Log-log plot of the total hopping rate, ν (in units of s^{-1}), as a function of temperature (in units of K). Experimental results are reproduced from Ref. 47 (solid curve), and are fit using Eq. (2.10) with $J(\omega)=\eta\omega^5$, $\omega_{\max}=5\times 10^{13}$ s^{-1} (i.e., Debye temperature of 400 K), $\eta=7.8$, and $t_0=0.03$ (i.e., a bare tunneling amplitude of 1 meV) (dashed curve).

Experiments on μ^+ diffusion in Al doped with Mn impurities[2] found no dependence of the μ^+ hopping rate on Mn concentration. We can therefore conclude that one-phonon processes due to site-energy asymmetries are not important in this system. The interstitial muon can occupy both the octahedral (O) and tetrahedral (T) sites in the fcc Al lattice. It is therefore possible to get a one-phonon contribution to the rate from intraunit-cell processes, *via* an O-T-O-T jump sequence. Previous studies[1,47] used this model in order to try and explain the linear temperature dependence of the μ^+ hopping rate, but it was concluded that this model was probably not applicable to this system.[1] We will use our model to try and explain the observed rate in terms of hopping between equivalent octahedral sites.

As shown in Fig. 5 the high-temperature results can be fit almost exactly by our model. We can also simultaneously account for the observed weaker temperature dependence in the intermediate temperature regime, although the fit is not as good as at higher temperatures. In making comparison with experiment we have multiplied the site-to-site rate given in Eq. (2.10) by 12. This is since the experiment measures the total muon jump rate, and each octahedral site has 12 nearest-neighbor octahe-

TABLE II. Parameters used to fit μ^+ in Al experimental data shown in Fig. 5. S is defined in Eq. (4.10) of the text.

η	S	t_0 (meV)	$\tilde{t}_0$ (meV)
6	0.75	0.8	0.38
8	1.0	1.0	0.37
10	1.25	1.3	0.37
11	1.375	1.5	0.38
12	1.5	1.7	0.38

dral sites to which the muon can hop.[47] The agreement shown in Fig. 5 could only be obtained using a narrow range of the parameters of the model. These values, given in Table II, agree well with previous estimates of the coupling strength and tunneling amplitude for μ^+ in Al.[1,2] For the purposes of comparison to previous work, the coupling strength η defined through Eq. (3.6) has also been reported in terms of an S value, defined by

$$\theta(T=0)=e^{-S} . \tag{4.10}$$

$\theta(T=0)$ is the lattice renormalizing factor, Eq. (2.8a), evaluated at zero temperature. For a 3D system described by an ω^5 spectral weight function, $S=\eta/8$. Previous studies have yielded S values of $S=1.73$ or 2.16 (Ref. 2) and $S=2.2$,[1] and a tunneling amplitude, t_0, of about 1 meV.[1,2] Using our model we have been able to fit the observed high-temperature hopping rates for μ^+ in Al using the true Debye temperature of the solid, $T_{\text{Debye}}=400$ K, and very reasonable values of the coupling strength, $S\approx 1$ ($\eta\approx 8$), and tunneling amplitude, $t_0\approx 1$ meV. Using the same S and t_0 we have also been able to account for the weaker temperature dependence seen at intermediate temperatures.

2. *Diffusion of muonium in KCL*

In Fig. 6 we show the experimentally determined hopping rate, i.e., site-to-site transfer rate, for muonium in KCl.[9] Stamp and Zang[48] have proposed a model of coherent impurity motion limited by one-phonon scattering to account for the observed temperature dependence. They assume that the delocalized impurity states are a good zero-order description, and calculate the rate of one-phonon scattering between these states. Within their model they conclude that there is no one-phonon scattering possible for impurities moving in narrow bands. Their one-phonon scattering rate is zero if the renormalized bandwidth is less than some threshold bandwidth, which is of the order of the Debye frequency of the lattice. However, for tunneling in narrow bands, i.e., systems with bandwidths very much less than the Debye frequency, the site-localized basis should be a better zero-order description and the analysis presented in this paper should be applicable. In their analysis Stamp and Zhang then proceed to find a T^3 temperature dependence for the one-phonon scattering rate, which is very different from our result. In the calculation of their impurity-lattice scattering rate, Stamp and Zhang have included only terms proportional to $n_{\mathbf{q}}$, the thermal average number of phonons in mode $\mathbf{q}$. These terms arise from a thermal

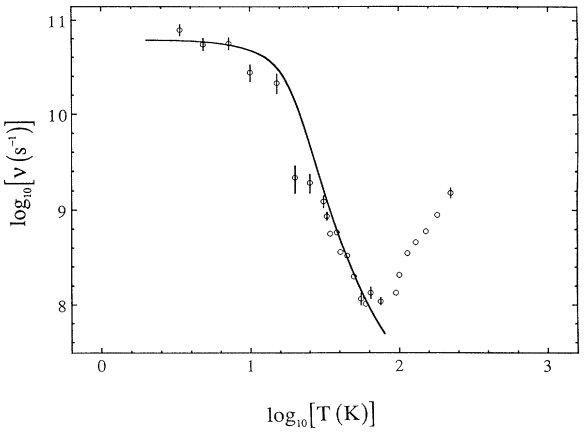

FIG. 6. Log-log plot of the muonium hopping rate, ν (in units of s^{-1}), as a function of temperature (in units of K). Experimental results are reproduced from Ref. 9, and are fit using $\nu=D/a^2$ with $J(\omega)=\eta\omega^5$, $\omega_{\max}=3\times 10^{13}$ s^{-1} (i.e., Debye temperature of 231 K), $\eta=13$, and $t_0=0.1$ (i.e., a bare tunneling amplitude of 2 meV). The theoretical results are shown as the solid curve and have been multiplied by $10^{-4.1}$ in order to scale to experiment (see text).

average of lattice correlation functions of the form $\langle b_{\mathbf{q}}^{\dagger} b_{\mathbf{q}} \rangle_{\text{bath}}$. They have omitted the terms proportional to $n_{\mathbf{q}}+1$, which arise from the lattice correlation functions $\langle b_{\mathbf{q}} b_{\mathbf{q}}^{\dagger} \rangle_{\text{bath}}$. If these terms are included, the resulting scattering rate shows a temperature dependence very similar to our one-phonon rate, i.e., constant at low temperatures and linear at higher temperatures. However, it is now no longer possible to explain the $T^{-3.3}$ temperature dependence found in the muonium in KCl experiment using only this one-phonon scattering.

We have tried to fit the experimental data within our model, by equating the experimentally observed hopping rate, ν, with the single-particle coherent diffusion coefficient, as was proposed by Stamp and Zhang.[48] That is $\nu=D/a^2$, with the coherent diffusion coefficient D given by[31,43]

$$D=\frac{a^2 2\tilde{t}_0^{\,2}}{z\gamma^- +\gamma^+} . \tag{4.11}$$

a is the distance between interstitial sites. Using Eq. (4.11) it was not possible to reproduce both the temperature dependence and the magnitude of the rate simultaneously. In Fig. 6, we show a representative fit to the data which reproduces the temperature dependence, i.e., $T^{-3.3}$, but is off by about 4 orders of magnitude in the absolute value of the rate. This could be due to the fact that simply interpreting the experimentally determined hopping rate as D/a^2 is not valid, as was discussed by Stamp and Zhang.[48] Alternatively, if other scattering mechanisms are important, for which there is some evidence,[8,9] these would act to reduce the coherent diffusion and hence reduce ν.[43]

Finally, we note one additional piece of quantitative evidence that can be interpreted as giving direct support

to our model. This is the observed flattening off in the rate for $T \leq 20$ K which is well reproduced by our results. In our analysis the temperature below which one-phonon scattering is dominant, kT^*, and the exponent, κ, of the power-law temperature dependence at higher temperatures $T^{-\kappa}$, are not independent. They are related through the ratio $\tilde{t}_0^2/\eta$ [Eqs. (3.14) and (3.15)]. Therefore given the $T^{-3.3}$ temperature dependence, our model would correctly predict that the hopping rate levels off below about 20 K.

V. CONCLUSIONS

In this paper we have proposed a new one-phonon scattering mechanism for impurities weakly coupled to the lattice and moving in narrow bands between identical interstitial sites. Previous studies have concluded that, in this physical situation, the lowest-order processes that can contribute to impurity-lattice scattering are two-phonon processes. The standard two-phonon scattering model predicts a very strong T^7 temperature dependence for the low-temperature transport properties of the interstitial in 3D. Such strong power-law temperature dependence has not been observed experimentally.[39] The one-phonon scattering rate derived here is constant at low temperatures and becomes linear in temperatures as the temperature is raised above the impurity bandwidth. At low temperatures this one-phonon contribution to the scattering is dominant and the high-order temperature dependence due to the two-phonon scattering is completely suppressed. We have given a quantitative estimate of when it should be possible to observe the standard two-phonon result.

In slightly different physical situations it is also possible to get one-phonon contributions to the rate. We have compared our one-phonon results to these other one-phonon mechanisms, arising either from tunneling between nondegenerate sites or from tunneling between inequivalent sites within a unit cell. Experimentally it should be possible to differentiate between these mechanisms, since the rates which they predict have different dependences on both temperature and sample purity.

The observed temperature dependence of the hopping rate of μ^+ in Al is well described by our model for intermediate and high temperatures. We have also attempted to explain the observed low-temperature hopping of muonium in KCl in terms of coherent diffusion, as has been previously proposed by Stamp and Zhang.[48] We found that within our model it was possible to fit the form of the observed temperature dependence but not the absolute magnitude. Some possible reasons for this discrepancy were presented.

The main conclusion of this paper is that the nonstationarity of the site-localized states can affect not only the coherent motion of an impurity but also the incoherent impurity-lattice scattering. When this effect is included we find that it is possible to get a one-phonon contribution to the impurity site-to-site transfer rate even for tunneling between degenerate states. At low temperatures this one-phonon contribution dominates, and the temperature dependence of the rate is very different from that predicted by the standard, two-phonon, analysis.

ACKNOWLEDGMENTS

We thank the ACS-PRF and NSD for financial support for this work. P.D.R. also thanks Eric Hiller for useful and fruitful discussions. K.B.W. would like to also thank the Alfred P. Sloan Foundation for financial support.

APPENDIX

In this appendix we outline the algebra involved in deriving the one- and two-phonon contributions to the rates when the $J_0^{2d}(2\tilde{t}_0\tau)$ factor is included in the evaluation of $F(\omega)$ given in Eq. (3.5). For a 3D tunneling system the exact $F(\omega)$ can be approximated by

$$F^{3D}(\omega)=\begin{cases}\dfrac{\exp\{-[(2/10)(\omega/\tilde{t}_0)]^2\}}{\tilde{t}_0\sqrt{2}}, & \omega<12\tilde{t}_0\ ,\\ 0, & \omega\geq 12\tilde{t}_0\ .\end{cases} \tag{A1}$$

This approximation is shown in Fig. 1(c), together with the exact function calculated by numerical integration of Eq. (3.5).

For a 3D tunneling system coupled to a 3D lattice, i.e., $F(\omega)$ given by Eq. (A1) and $J(\omega)$ given by Eq. (3.6) with $n=5$, the one-phonon rate, valid for $12\tilde{t}_0 \leq 1$, is given by

$$\gamma^{(1)}=\frac{\eta}{\tilde{t}_0\sqrt{2}}(2kT)^4\int_0^{12\tilde{t}_0/2kT} dx\, x^3\coth(x) \times e^{-[(4/10)(kT/\tilde{t}_0 x]^2}\ . \tag{A2}$$

For $kT \ll 6\tilde{t}_0$ we can take the upper limit of the integral to infinity, expand the Gaussian in a power series in $(4/10)(kT/\tilde{t}_0)x$, and use[49]

$$\lim_{y\to\infty}\int_0^y dx\, x^n\coth(x)\sim(\tfrac{1}{2})^n n!\zeta(n+1)+\frac{y^{n+1}}{n+1} \tag{A3}$$

to evaluate the resulting integrals. $\zeta(n)$ is the Riemann ζ function. Including only the leading-order term gives the low-temperature limit of Eq. (3.11). The high-temperature limit of $\gamma^{(1)}$ is obtained upon replacing $\coth(x)$ in Eq. (A2) by its leading-order term, $1/x$.

The major contribution to the two-phonon rate is given by

$$\gamma^{(2)}\sim\eta^2\tfrac{5}{4}\sqrt{\pi/2}(2kT)^7\int_0^{1/2kT} d\omega\frac{\omega^6}{\sinh^2(\omega)}\ , \tag{A4}$$

which is the same as the δ-function approximation, Eq. (3.8), with $\pi/2$ replaced by $1.25\sqrt{\pi/2}$. We ignore this small difference and use the δ-function approximation to $\gamma^{(2)}$ given in Eq. (3.8) for the two-phonon rate.

Finally we summarize the results for a 2D tunneling system coupled to a 2D lattice, i.e., $F(\omega)$ given in Fig. 1(b) and $J(\omega)$ given by Eq. (3.6) with $n=4$. The one- and two-phonon contributions to the rate are given by[43]

$$\gamma^{(1)}\approx\begin{cases}\eta^2\left[\dfrac{\tilde{t}_0}{\eta}\right]\tilde{t}_0 0.9\tfrac{128}{3}, & kT\ll 4\tilde{t}_0\ ,\\ \eta^2\left[\dfrac{\tilde{t}_0}{\eta}\right]0.9\tfrac{64}{3}kT, & kT\gg 4\tilde{t}_0\ ,\end{cases} \tag{A5}$$

and

$$\gamma^{(2)} \approx \begin{cases} \eta^2 \dfrac{(2\pi)^5}{60}(kT)^5, & 2kT \ll 1 , \\ \eta^2 \dfrac{2\pi}{3}(kT)^2, & 2kT \geq 1 . \end{cases} \tag{A6}$$

From these expressions we see that, for temperatures greater than the bandwidth, the temperature dependence is completely determined by the ratio t_0/η and scales as η^2. The transition temperature also depends on t_0/η and is given by[43]

$$kT^* \approx \begin{cases} \left[\dfrac{\tilde{t}_0}{\eta} \right]^{1/4} 0.585\,65, & 2kT^* \ll 1 , \\ \dfrac{\tilde{t}_0}{\eta} 9.167\,32, & 2kT^* \geq 1 . \end{cases} \tag{A7}$$

In the intermediate-temperature regime, $kT^* \leq kT \leq 2.5kT^*$, the temperature dependence of the rate is well described by $\gamma^- \sim T^\kappa$ with κ given by

$$\kappa \approx \begin{cases} -\log_{10}(\tilde{t}_0/\eta), & \tilde{t}_0/\eta \geq 10^{-5} , \\ 5, & \tilde{t}_0/\eta < 10^{-5} . \end{cases} \tag{A8}$$

*Current address: Department of Chemistry, University of Wisconsin at Madison, Madison, WI 53706.

[1]O. Hartmann, E. Karlsson, E. Wackelgard, R. Wappling, D. Richter, R. Hempelmann, and T. O. Niinikoski, Phys. Rev. B **37**, 4425 (1988).
[2]K. W. Kehr, D. Richter, J.-M. Welter, O. Hartmann, E. Karlsson, L. O. Norlin, T. O. Niinikoski, and A. Yaouanc, Phys. Rev. B **26**, 567 (1982).
[3]R. Kadono, J. Imazato, T. Matsuzaki, K. Nishiyama, D. Richter, and J.-M. Welter, Phys. Rev. B **39**, 23 (1989).
[4]J. H. Brewer, M. Celio, D. R. Harshman, R. KEitel, S. R. Kreitzman, G. N. Luke, D. R. Noakes, R. E. Turner, E. J. Ansaldo, C. W. Clawson, K. M. Crowe, and C. Y. Huang, Hyperfine Interact. **31**, 191 (1986).
[5]R. Kadono, J. Imazato, K. Nishiyama, K. Nagamine, T. Yamazaki, D. Richter, and J.-M. Welter, Phys. Lett. **109A**, 61 (1985).
[6]R. Kadono, J. Imazato, K. Nishiyama, K. Nagamine, T. Yamazaki, D. Richter, and J.-M. Welter, Hyperfine Interact. **17**, 109 (1984).
[7]E. Yagi, G. Flik, K. Furderer, N. Haas, D. Herlach, J. Major, A. Seeger, W. Jacobs, M. Krause, M. Krauth, H.-J. Mundinger, and H. Orth, Phys. Rev. B **30**, 441 (1984).
[8]R. Kadono, R. F. Kiefl, E. J. Ansaldo, J. H. Brewer, M. Celio, S. R. Kreitzman, and G. M. Luke, Phys. Rev. Lett. **64**, 665 (1990).
[9]R. F. Kiefl, R. Kadono, J. H. Brewer, G. M. Luke, H. K. Yen, M. Celio, and E. J. Ansaldo, Phys. Rev. Lett. **62**, 792 (1989).
[10]I. S. Anderson, N. F. Berk, J. J. Rush, T. J. Udovic, R. G. Barnes, A. Magerl, and D. Richter, Phys. Rev. Lett. **65**, 1439 (1990).
[11]D. Steinbinder, H. Wipf, A. Magerl, D. Richter, A.-J. Dianoux, and K. Neumaier, Europhys. Lett. **6**, 535 (1988).
[12]A. Weidinger and R. Peichl, Phys. Rev. Lett. **54**, 1683 (1985).
[13]Z. Qi, J. Volkl, R. Lasser, and H. Wenzl, J. Phys. F **13**, 2053 (1983).
[14]N. S. Sullivan, D. Zhou, M. Rall, and C. M. Edwards, Phys. Lett. A **138**, 329 (1989).
[15]D. Zhou, C. M. Edwards, and N. Sullivan, Phys. Rev. Lett. **62**, 1528 (1989).
[16]G. Nunes, Jr., C. Jin, A. M. Putnam, and D. M. Lee, Phys. Rev. Lett. **65**, 2149 (1990).
[17]D. Candela, D. R. McAllaster, L.-J. Wei, and G. A. Vermeulen, Phys. Rev. Lett. **65**, 595 (1990).
[18]A. R. Allen, M. G. Richards, and J. Schratter, J. Low Temp. Phys. **47**, 289 (1982).
[19]X. D. Zhu, A. Lee, A. Wong, and U. Linke, Phys. Rev. Lett. **68**, 1862 (1992).
[20]C.-H. Hsu, B. E. Larson, M. El-Batanouny, C. R. Willis, and K. M. Martinin, Phys. Rev. Lett. **66**, 3164 (1991).
[21]T.-S. Lin and R. Gomer, Surf. Sci. **255**, 41 (1991).
[22]S. C. Wang and R. Gomer, J. Chem. Phys. **83**, 4193 (1985).
[23]M. Tringides and R. Gomer, Surf. Sci. **155**, 254 (1985).
[24]C. Dharmadhikari and R. Gomer, Surf. Sci. **143**, 223 (1984).
[25]R. Difoggio and R. Gomer, Phys. Rev. B **25**, 3490 (1982).
[26]T. Holstein, Ann. Phys. **8**, 325 (1959).
[27]C. P. Flynn and A. M. Stoneham, Phys. Rev. B **1**, 3966 (1970).
[28]Y. Kagan and M. I. Klinger, J. Phys. C **7**, 2791 (1974).
[29]D. Emin, M. I. Baskes, and W. D. Wilson, Phys. Rev. Lett. **42**, 791 (1979).
[30]R. Silbey and R. A. Harris, J. Phys. Chem. **93**, 7062 (1989).
[31]K. Kitahara, H. Metiu, J. Ross, and R. Silbey, J. Chem. Phys. **65**, 2871 (1976).
[32]S. Efrima and H. Metiu, J. Chem. Phys. **69**, 2286 (1978).
[33]I. C. da Cunha Lima, A. Troper, and S. C. Ying, Phys. Rev. B **41**, 11 798 (1990).
[34]P. D. Reilly, R. A. Harris, and K. B. Whaley, J. Chem. Phys. **95**, 8599 (1991).
[35]J. W. Allen and R. Silbey, Chem. Phys. **43**, 341 (1979).
[36]D. Yarkony and R. Silbey, J. Chem. Phys. **65**, 1042 (1976).
[37]D. Yarkony and R. Silbey, J. Chem. Phys. **67**, 5818 (1977).
[38]M. Grover and R. Silbey, J. Chem. Phys. **54**, 4843 (1971).
[39]Y. Fukai and H. Sugimoto, Adv. Phys. **34**, 263 (1985).
[40]H. Teichler and A. Seeger, Phys. Lett. **82A**, 91 (1981).
[41]G. D. Mahan, *Many Particle Physics,* 2nd ed. (Plenum, New York, 1990), Sec. 6.2.
[42]R. W. Zwanzig, *Lectures in Theoretical Physics* (Colorado Associated University Press, Boulder, 1960), Vol. 3, p. 106.
[43]P. D. Reilly, Ph.D. thesis, University of California at Berkeley, 1992.
[44]J. Kondo, Hyperfine Interact. **31**, 117 (1986).
[45]I. S. Gradshetyn and I. M. Ryzhik, *Table of Integrals, Series and Products,* 4th ed. (Academic, Orlando, 1980), p. 352.
[46]I. S. Gradshetyn and I. M. Rhyzik, *Tables of Integrals, Series and Products* (Ref. 45), p. 732.
[47]D. Richter, Hyperfine Interact. **31**, 169 (1986).
[48]P. C. E. Stamp and C. Zhang, Phys. Rev. Lett. **66**, 1902 (1991).
[49]I. S. Gradshetyn and I. M. Ryzhik, *Tables of Integrals, Series, and Products* (Ref. 45), p. 325.